An Experimental and Computational Study of the Kinetics and Mechanism of the Reaction of Methyl Formate with Cl Atoms

David A. Good, Jaron Hansen, Mike Kamoboures, Randy Santiono, and Joseph S. Francisco*

Department of Chemistry and Department of Earth and Atmospheric Science, Purdue University, West Lafayette, Indiana 47907-1393

Received: July 20, 1999; In Final Form: October 29, 1999

Ab initio molecular orbital theory has been used to examine the kinetics and mechanism for the reaction of chlorine atoms with methyl formate. From the ab initio parameters, the room-temperature rate constant is calculated and found to be in reasonable agreement with the experimental determination. It is found that 90% of the reaction proceeds via abstraction of the carbonyl hydrogen from methyl formate by chlorine atoms, resulting in the formation of CH_3OCO radical.

I. Introduction

Concerns about mobile source emissions and their impact on urban tropospheric ozone formation have spurred research into alternative fuels with the goal of reducing emissions of CO and NO_x. Fuel composition affects the tendency of a fuel to form soot particulates and NO_x. Increasing the carbon-to-hydrogen ratio or the number of carbon−carbon bonds increases the tendency of a fuel to form soot. Oxygenated hydrocarbons such as ethers can be added to fuels to maintain performance while lowering tailpipe emissions of CO.[1] Dimethyl ether (DME) is a fuel anti-knock agent and proposed diesel fuel substitute. DME has been used as a methanol ignition improver in diesel engines, where it has been reported to reduce hydrocarbon emissions.[1] Some of its attractive features include low self-ignition temperature, low octane number (high cetane number, 55−60), and reduced combustion noise, particle emission, and NO_x emissions. DME fueled engines are nonsooting, and DME can be economically produced from a one-step synthesis.[1] The atmospheric oxidation of DME has been studied by Japar et al.,[2] Jenkin et al.,[3] Wallington et al.,[4] Langer et al.,[5] and Sehested et al.[6,7]

Japar et al.[2] used $Cl^{\bullet}$ atom initiated hydrogen abstraction to simulate the reaction of DME with tropospheric OH radical in the presence of NO. Reaction products were determined using FTIR spectroscopy. The production of methyl formate accompanied the loss of dimethyl ether quantitatively. The yield of methyl formate relative to DME loss was found to be 0.90.[2] To the best of our knowledge, the resulting fate of methyl formate has not been studied. This work addresses the atmospheric oxidation of methyl formate. Figure 1 shows a proposed mechanism for the atmospheric oxidation of methyl formate. The first step is a hydrogen abstraction reaction initiated by chlorine atom. As shown there are two possible reaction pathways, hydrogen abstraction of one of the methyl hydrogens or hydrogen abstraction of the carbonyl hydrogen. It is a goal of this work to determine the branching ratio for this step.

II. Methods

A. Experimental Methods. Gas mixtures of chlorine, oxygen, and methyl formate were introduced into a 64 cm^3 square Teflon reaction vessel at various concentrations. Gas pressures were monitored using a MKS baritron capacitance manometer which is accurate to ±0.01 Torr. The mixture was allowed to equilibrate for over 1 h. Chlorine was photolyzed from the output of a Xenon arc lamp. A 330 nm cutoff filter was used to limit the amount of UV light that entered the cell and thus decrease the potential for photolysis side reactions. The reaction progress was monitored via FTIR spectroscopy using a Matteson Instruments Galaxy 7020 series spectrometer. The spectrometer was operated in the mid-IR at 1 cm^{-1} resolution with an 18 cm path length. The resulting spectra are the average of 64 replicate scans. As a test of the effectiveness of the cutoff filter at limiting photolysis side reactions, methyl formate was radiated in the presence of all reactants except chlorine. No appreciable loss of methyl formate was found over the time period of typical experiments. Methyl formate (99.9%) was purchased from Aldrich and was subjected to several freeze−pump−thaw cycles prior to use. No impurities were detected using FTIR and GC/MS. Ultrahigh purity oxygen (99.99%) was purchased from AGA Speciality Gases, while ultrahigh purity chlorine (99.97%) was purchased from Scott Specialty Gases. Both reagents were used without further purification. Typical experimental conditions consist of 500 mTorr of CH_3OCOH, 500 mTorr of Cl_2 and 20 Torr of O_2.

B. Computational Methods. All calculations were performed with the GAUSSIAN 94 package of programs.[8] Geometry optimizations for all species were carried out for all structures to better than 0.001 Å for bond lengths and 0.1° for angles. The geometries were fully optimized, and with these geometries a frequency calculation was performed. Optimizations and frequency calculations were performed using the second-order Moller−Plessant perturbation method (MP2) with the 6-311++G(2d,2p) basis set. In addition, single-point energies were calculated using the QCISD(T) method with the same basis set. Restricted wave functions were used for closed-shell and unrestricted wave functions for open-shell systems with all orbitals active. For each species, the degree of spin contamination was monitored. For doublet systems, the $\langle s^2 \rangle$ value did not exceed 0.78, thus indicating that the wave functions were not significantly contaminated by higher order spin states. To obtain the energy at 298 K, the thermal energy of each species was added to its total energy instead of the zero-point energy (ZPE). Usually vibrational frequencies calculated at the MP2 level are found to overestimate experimental anharmonic frequencies and thus zero-point energies. To correct for this overestimation, a popular approach has been to scale the ZPE. The vibrational

10.1021/jp992478z CCC: $19.00
Published on Web 02/02/2000

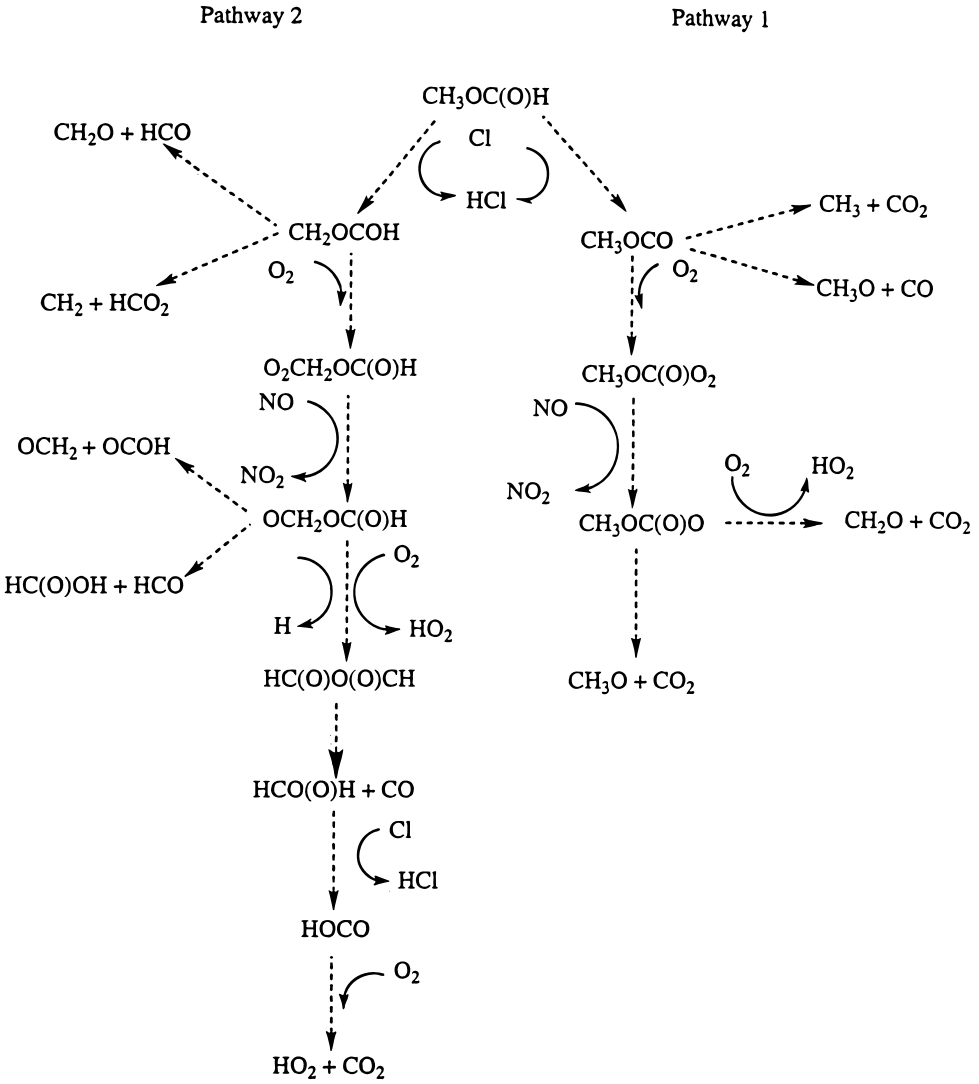

Figure 1. Proposed methyl formate oxidation mechanism.

frequencies and ZPE values used in this work have been scaled by the recommended value of 0.97.[28]

Results and Discussion

A. Relative Rate Method For Rate Constant Measurement. To calibrate our experimental method, we measured the rate of Cl reaction with methyl formate using a relative rate technique. In this experiment, mixtures of methyl formate (~0.5 Torr), reference gas (CH_2Cl_2, CH_3F, CH_2F_2; ~2 Torr), and Cl_2 (excess) were allowed to equilibrate for 1 h. The mixture was illuminated at wavelengths > 330 nm to produce chlorine radicals and initiate the reaction. The reactant concentrations were monitored using FTIR spectroscopy by observing the decrease in intensity of one of their spectral features. The rate for chlorine atom reaction with methyl formate was measured relative to CH_3F, CH_2Cl_2, and CH_2F_2. For CH_3F, the recommended[9] reaction rate is $3.5 \pm 1.3 \times 10^{-13}$ cm^3 molecule^{-1} s^{-1} which comes from the work of Tschuikow-Roux et al.,[10] Tuazon et al.,[11] Wallington et al.,[12] and Manning et al.[13] For CH_2Cl_2, the recommended value of $3.3 \pm 1.3 \times 10^{-13}$ cm^3 molecule^{-1} s^{-1} is derived from the relative rate work of Tschuikow-Roux et al.,[11] as recommended by the JPL publication.[9] This work shows good agreement with the direct measurements of Niki et al.[14] and Beichert et al.[15] CH_2F_2 is the slowest species of the three to react with chlorine, having a recommended reaction rate of $7.0 \pm 2.1 \times 10^{-14}$ cm^3 molecule^{-1} s^{-1} based on the work of Tschuikow-Roux et al.[9,26] The 298 K rate constant for reaction of Cl atoms with each of the above reference species is listed in Table 1, column 2. All reference reagents were found to react slower than methyl formate with chlorine. Example experiments from a set of three replicate determinations are shown in Figure 2. The relative rate of the reference species reacting with chlorine to that of methyl formate reacting with chlorine, k_r/k_m, is listed in Table 1, column 3. The reported ratio is the average of the three replicates, while reported errors represent 2σ from the least-squares fit. The rate constant for reaction of methyl formate with chlorine atoms is presented in the final column of Table 1. With respect to dichloromethane, a ratio $k_{CH_2Cl_2}/k_{CH_3OCOH}$ of 0.23 ± 0.01 was determined. Using a rate constant for CH_2Cl_2 reaction with

TABLE 1: Relative Rates for Methyl Formate Reaction with Chlorine Atoms[a]

reference species	k_r reference reaction with Cl	k_r/k_m	k_m methyl formate reaction with Cl
CH_3F	$(3.5 \pm 1.3) \times 10^{-13}$	0.22 ± 0.01	$(1.60 \pm 0.58) \times 10^{-12}$
CH_2Cl_2	$(3.3 \pm 1.3) \times 10^{-13}$	0.23 ± 0.01	$(1.43 \pm 0.67) \times 10^{-12}$
CH_2F_2	$(7.0 \pm 2.1) \times 10^{-14}$	0.06 ± 0.001	$(1.17 \pm 0.33) \times 10^{-12}$
average			$(1.4 \pm 0.5) \times 10^{-12}$

[a] All rate data at 298 K. All rate constants in units of cm^3 molecule^{-1} s^{-1}.

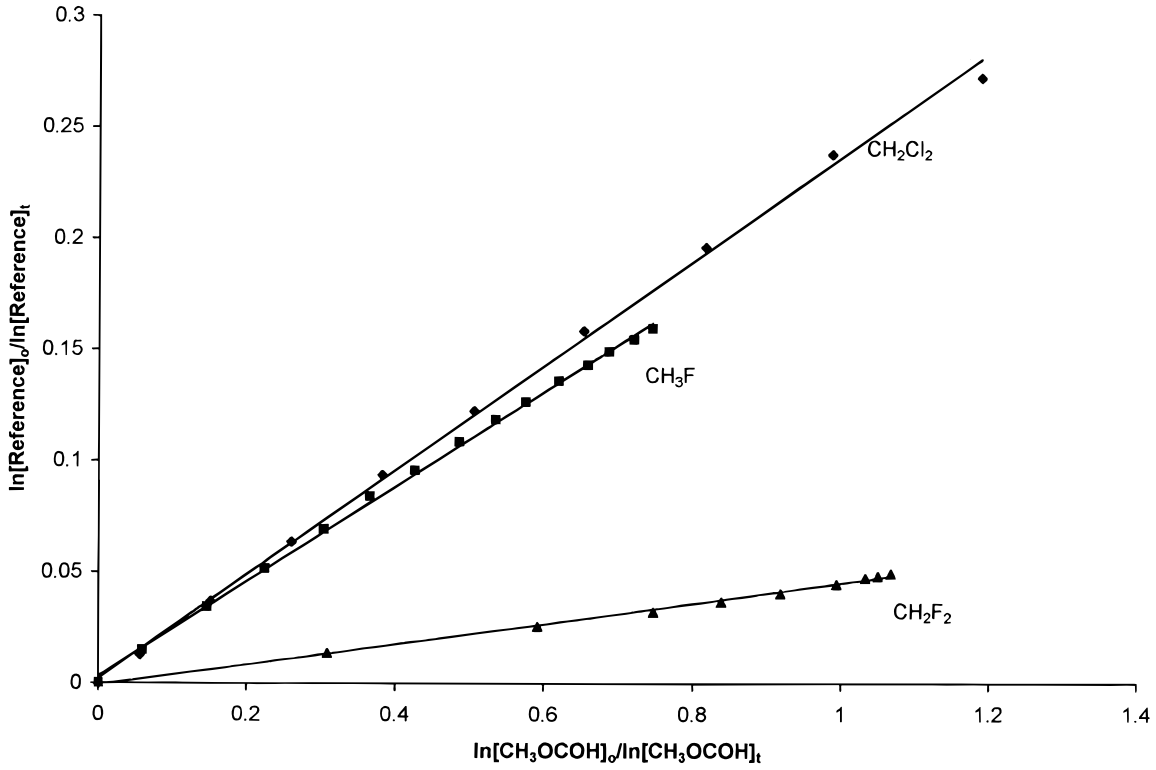

Figure 2. Relative rates of reference vs methyl formate expressed as k_r/k_m.

chlorine of $(3.3 \pm 1.3) \times 10^{-13}$ cm^3 molecule^{-1} s^{-1}, a value for the rate constant for methyl formate reacting with Cl is found to be $(1.43 \pm 0.67) \times 10^{-12}$ cm^3 molecule^{-1} s^{-1}. For fluoromethane, a ratio of k_{CH_3F}/k_{CH_3OCOH} of 0.22 ± 0.01 was determined thus yielding a methyl formate reaction rate of $(1.60 \pm 0.58) \times 10^{-12}$ cm^3 molecule^{-1} s^{-1}. For CH_2F_2, a rate constant of $(1.17 \pm 0.33) \times 10^{-12}$ cm^3 molecule^{-1} s^{-1} is determined. These separate determinations yield an average rate constant of $(1.4 \pm 0.5) \times 10^{-12}$ cm^3 molecule^{-1} s^{-1} for methyl formate reacting with Cl. Two previous investigators have measured the rate of methyl formate reaction with chlorine. Wallington et al.,[16] using a relative rate technique, found a rate constant of $(1.4 \pm 0.1) \times 10^{-12}$ cm^3 molecule^{-1} s^{-1}. Recently, Notario et al.[17] used a pulsed laser photolysis-resonance fluorescence technique to directly measure the 298 K rate constant by following the loss of chlorine atoms in the presence of methyl formate. The rate constant was determined to be $(1.8 \pm 0.2) \times 10^{-12}$ cm^3 molecule^{-1} s^{-1}. Our value of $(1.4 \pm 0.5) \times 10^{-12}$ cm^3 molecule^{-1} s^{-1} is in agreement with the measurements of Wallington et al.[16] and Notario et al.[17]

B. Reaction Products. Figure 3a shows an FTIR spectrum of methyl formate in the presence of oxygen and chlorine prior to photolysis and thus only features due to methyl formate are present. Shortly after photolysis is initiated, absorption features due to HCl, CO_2, and CO are clearly visible. At later times, features due to formic acid anhydride and formic acid become evident. For formic acid anhydride, the two CO stretches at 998 and 1105 cm^{-1} as well as the C═O stretches at 1822 and 1767 cm^{-1} are present.[18−20] For formic acid, the CO stretch also at 1105 cm^{-1} as well as the C═O stretch at 1776 cm^{-1} are visible. Formic acid anhydride and formic acid are products from the reaction channel in which a hydrogen atom is abstracted from the CH_3 group of methyl formate (Figure 1, pathway 2). The decomposition of formic acid anhydride (FAA) has been studied by Lundell et al.[19] and Kuhne et al.[20] Lundell et al.[19] using ab initio methodology confirmed the primary dissociation pathway for FAA is production of formic acid and CO. Kuhne et al.[20] determined a time constant for the rearrangement of formic acid anhydride to formic acid and CO of roughly 1 h. Cl radical initiated decomposition of formic acid has been studied by Tyndall et al.[21] who determined the primary (∼96%) dissociation pathway is removal of the carbonyl hydrogen in formic acid to form the HOCO radical. The HOCO radical reacts with O_2 to yield HO_2 and CO_2.

No evidence for the second degradation channel (Figure 1, pathway 1) of methyl formate is found. This channel should produce products such as CH_2O, CH_3, and CH_3O. Under oxygen-rich conditions, CH_3 and CH_3O should also yield formaldehyde. No evidence for CH_2O exists. The reaction of CH_3O radicals with O_2 to form CH_2O is very slow, having a recommended rate constant[9] of 1.9×10^{-15} cm^3 molecule^{-1} s^{-1}. The subsequent reaction of formaldehyde with excess chlorine radicals by contrast is relatively fast, having a rate constant of 7.3×10^{-11} cm^3 molecule^{-1} s^{-1}. In contrast to formaldehyde, formic acid is removed more slowly by chlorine radicals. A rate constant of 2.3×10^{-13} cm^3 molecule^{-1} s^{-1} is recommended.[9,21] The fact that formic acid is detected as a degradation product while formaldehyde is not may be explained by arguing that formaldehyde is rapidly reacted away by excess chlorine radicals. Thus, the concentration of formaldehyde never increases above the detection limits of the method.

Both pathways in Figure 1 contribute to the loss of methyl formate and to the rate constant determined in the previous section. To estimate the relative importance (i.e., branching ratio) of each pathway, the individual rate constants for each pathway were calculated using ab initio molecular orbital methods.

C. Computational Study of the Mechanism of Cl Atom Reaction with Methyl Formate. *1. Structure and Energetics.* The structures of methyl formate, the two possible transition states, and the two alkyl radical products are illustrated in Figure 4. The two C−O single bonds are predicted to be 1.441 and

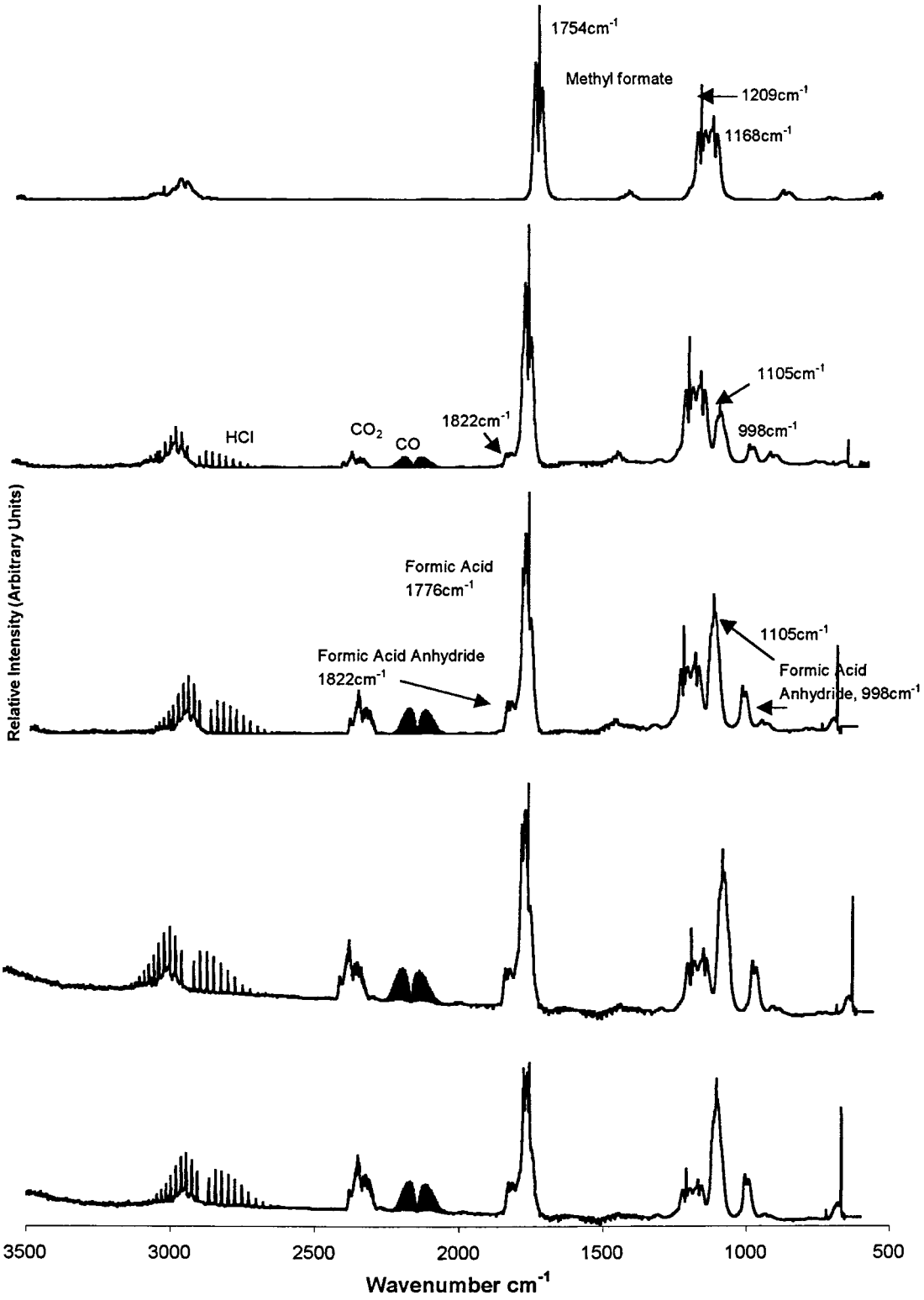

Figure 3. Reaction progress for the reaction, $CH_3OCOH + Cl \rightarrow$ products.

1.341 Å, while the carbonyl bond is predicted to be 1.207 Å in length. The experimentally determined values reported by Curl[22] are 1.437, 1.334, and 1.200 Å, respectively. Thus, the error associated with the present methodology is less than 1%.

Figure 4b shows the transition state in which the carbonyl hydrogen is removed by atomic chlorine. In the transition state, the carbonyl C−H bond lengthens to 1.208 Å while the forming H−Cl bond shortens to 1.621 Å. In addition, calculations at the MP2/6-311++G(2d,2p) level of theory suggest that the carbonyl C═O bond shortens from 1.207 Å in methyl formate to 1.193 Å in the transition state. The C−O single bond adjacent to the methyl group increases from 1.441 Å in methyl formate to 1.454 Å in the transition state. In contrast, the C−O single bond adjacent to the carbonyl center decreases to 1.318 Å.

Figure 4c illustrates the removal of one of the longer, out-of-plane hydrogen atoms of the methyl group. In this transition state, the cleaving C−H bond lengthens to 1.302 Å while the H−Cl bond shortens to 1.501 Å. Extraction of the in-plane hydrogen atom was found to lie approximately 5 kcal mol^{-1} higher in energy than the transition state involving the out-of-

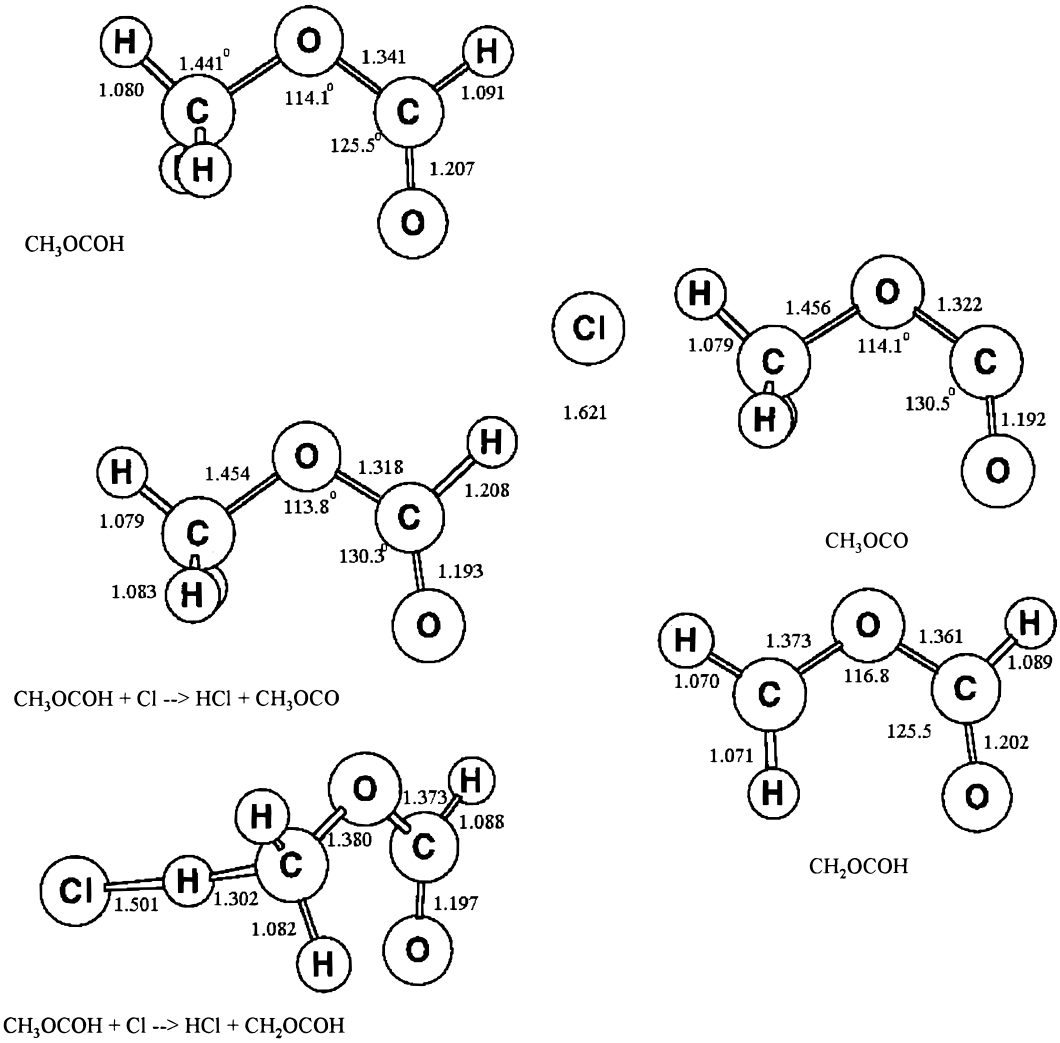

Figure 4. MP2/6-311++G(2d,2p) optimized structure of methyl formate, transition states, and alkyl radical products.

TABLE 2: Energetic Parameters for Methyl Formate, Transition States, and Products at 298 K[a]

species	energy QCISD(T)/6-311++G(2d,2p)	thermal correction	partition function	imaginary frequency
CH_3OCOH	−228.6425578	0.0656	4.653×10^{31}	
$Cl-CH_3OCOH$	−688.2589126	0.0605	1.028×10^{34}	−1070
$CH_3OCOH-Cl$	−688.2628421	0.0617	1.066×10^{34}	−860
Cl	−459.625946	.0014	4.00×10^{26}	
CH_3OCO	−227.9780063	0.0531		
CH_2OCOH	−227.9746316	0.0511		
HCl	−460.2886755	.00899		

[a] Energies and thermal corrections in hartrees. Partition functions in units of cm^3 $molecule^{-1}$ s^{-1}. Imaginary frequencies in units of cm^{-1}.

plane hydrogen atoms. Extraction of the in-plane hydrogen atom will not contribute significantly to the overall rate constant. Parts d and e of Figure 4 present the optimized structure of the alkyl radicals, CH_3OCO and CH_2OCOH.

The relevant energetic parameters for each reactant and transition state are reported in Table 2 and Figure 5. For the following reactions, removal of the carbonyl hydrogen is predicted to be favored both thermodynamically and kinetically:

$$CH_3OCOH + Cl \rightarrow CH_3OCO + HCl \quad (1a)$$

$$CH_3OCOH + Cl \rightarrow CH_2OCOH + HCl \quad (1b)$$

At the QCISD(T)/6-311++G(2d,2p)//UMP2/6-311++G(2d,2p) level of theory, the reaction enthalpy for removal of the carbonyl hydrogen is slightly more favorable having a reaction enthalpy of −2.0 kcal mol^{-1}, while the removal of a methyl hydrogen (reaction 1b) is calculated to be exothermic by −1.1 kcal mol^{-1}. Using G2 and G2(MP2) methodology along with isodesmic reactions, Good et al.[25] determined the 298 K heat of formation of CH_3OCO and CH_2OCOH to be −37.5 and −36.5 kcal mol^{-1}, respectively. These values along with literature values for the 298 K heats of formation of methyl formate (−85.0 kcal mol^{-1}),[24] HCl (−22.06),[9] and Cl (28.9)[9] yield reaction enthalpies for reactions 1a and 1b of −3.5 and −2.5 kcal mol^{-1}, respectively. These values are in good agreement with the values determined in this work.

The C−H bond dissociation energy (BDE) can be estimated by using 298 K enthalpy values for each species in reactions 2a and 2b.

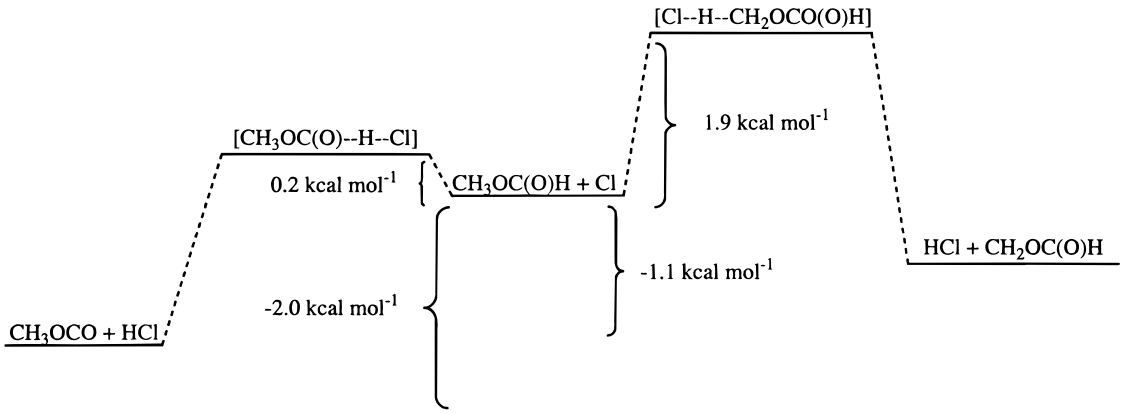

Figure 5. Relative energetics for methyl formate reactions.

$$CH_3OCOH \rightarrow CH_3OCO + H \quad (2a)$$

$$CH_3OCOH \rightarrow CH_2OCOH + H \quad (2b)$$

The 298 K heat of formation[9] of the hydrogen atom is 52.1 kcal mol^{-1}. Thus, the BDE for reactions 2a and 2b is estimated to be 99.6 and 100.6 kcal mol^{-1}, respectively. Previous investigators have noted a correlation between a molecule's C−H bond dissociation energy and the reaction rate of CH bond dissociation reactions.[27] In addition to being thermodynamically favored, our analysis suggests that removal of the carbonyl hydrogen is also kinetically favored over removal of one of the methyl hydrogen atoms. This suggestion is supported by our molecular orbital calculations of the activation energies for pathways 1 and 2. At the QCISD(T)/6-311++G(2d,2p)//UMP2/6-311++G(2d,2p) level of theory, removal of the carbonyl hydrogen is calculated to proceed over a reaction barrier of 0.2 kcal mol^{-1} while the activation energy for removal of a methyl hydrogen is a substantially higher 1.9 kcal mol^{-1}.

2. Comparison of Branching Ratio and Rate Constant from Theory and Experiment. For reactions 1a and 1b, the branching ratio is expressed as the ratio of the rate constants, i.e., k_{1a}/k_1. From transition state theory, each rate constant is given by the following expression:

$$k = \frac{Lk_bT}{h}\frac{Q^{\ddagger}}{Q_{Cl}Q_{methylformate}} e^{-E_a/k_bT} \quad (3)$$

where E_a is the activation energy, T is the temperature, Q represents the total partition function incorporating translational, rotational, vibrational, and electronic terms ($Q_T = Q_eQ_vQ_rQ_t$), L is a statistical factor representing the number of equivalent extractable hydrogen atoms, and k_b is Boltzmann's constant. Tunneling corrections, which may slightly lower the activation energy, have not been included in this work. Removal of a methyl hydrogen is estimated to have a rate constant of 2.8×10^{-13} cm^3 molecule^{-1} s^{-1}, while removal of the carbonyl hydrogen is predicted to have a rate constant of 2.5×10^{-12} cm^3 molecule^{-1} s^{-1} at 298 K. The combined rate constant is thus 2.8×10^{-12} cm^3 molecule^{-1} s^{-1}. The experimentally determined rate[16,17] has previously been found to range between 1.4×10^{-12} and 1.8×10^{-12} cm^3 molecule^{-1} s^{-1}. Thus, the 298 K rate constant for the reaction of methyl formate with chlorine atom as determined by our ab initio methodology is a reasonable estimate. It is also reasonable to expect the branching ratio of reactions 1a and 1b to be more reliable, as errors common to both calculations may cancel.

Using the above rate data for reactions 1a and 1b, it is predicted that 90% of the total reaction proceeds through reaction 1a resulting in the formation of CH_3OCO radical. A reasonable estimate for the uncertainty associated with the computation of each activation energy is ±0.5 kcal mol^{-1}. With this uncertainty, the ratio k_{1a}/k_1 could range from 65% to 97%. Bartels et al.[23] examined the analogous hydrocarbon system, i.e.,

$$CH_3CHO + Cl \rightarrow CH_3CO + HCl \quad (4a)$$

$$CH_3CHO + Cl \rightarrow CH_2CHO + HCl \quad (4b)$$

Their investigation determined k_{4b}/k_{4a} to be 0.0753 and thus k_{4a}/k_4 to be over 92%. Thus, for the acetylaldehyde system, removal of the carbonyl hydrogen is shown to be favored over abstraction of a methyl hydrogen. The analogous conclusions are suggested for the methyl formate system.

IV. Conclusions

FTIR analysis of the products from the reaction of chlorine atoms with methyl formate show that both formic acid anhydride and formic acid are products of the reaction. Chlorine radical initiated hydrogen abstraction of methyl formate is found to occur with a rate of $1.4 \pm 0.5 \times 10^{-12}$ cm^3 molecule^{-1} s^{-1}. This value is in agreement with previous determinations by Wallington et al.[16] ($1.4 \pm 0.1 \times 10^{-12}$ cm^3 molecule^{-1} s^{-1}) and Notorio et al.[17] ($1.8 \pm 0.2 \times 10^{-12}$ cm^3 molecule^{-1} s^{-1}). Ab initio calculations at the QCISD(T)/6-311++G(2d,2p)//MP2/6-311++G(2d,2p) level of theory predict the rate to be 2.8×10^{-12} cm^3 molecule^{-1} s^{-1}, which is in reasonable agreement with experimental determinations. Additionally, our calculations suggest that the reaction between methyl formate and chlorine occurs predominately (90%) at the carbonyl hydrogen resulting in the formation of CH_3OCO radical.

References and Notes

(1) Rouhi, A. M. *Chem Eng. News* **1985**, *44*, 37.
(2) Japar, S. M.; Wallington, T. J.; Richert, J. F. O.; Ball, J. C. *Int. J. Chem. Kinet*. **1990**, *22*, 1257.
(3) Jenkin, M. E.; Hayman, G. D.; Wallington, T. J.; Hurley, M. D.; Ball, J. C.; Nielsen, O. J.; Ellerman, T. *J. Phys. Chem*. **1993**, *97*, 11712.
(4) Wallington, T. J.; Hurley, M. D.; Ball, J. C.; Jenkin, M. E. *Chem. Phys. Lett*. **1993**, *211*, 41.
(5) Langer, S.; Ljungstrom, E.; Ellerman, T.; Nielsen, O. J.; Sehested, J. *Chem. Phys. Lett*. **1995**, *240*, 53.
(6) Sehested, J.; Mogelberg, T.; Wallington, T. J.; Kaiser, E. W.; Nielsen, O. J. *J. Phys. Chem*. **1996**, *100*, 17218.
(7) Sehested, J.; Sehested, K.; Platz, J.; Egsgaard, H.; Nielsen, O. J. *Int. J. Chem. Kinet*. **1997**, *29*, 627.
(8) Frisch, M. J.; Trucks, G. W.; Schlegel, H. B.; Gill, P. M. W.; Johnson, B. G.; Robb, M. A.; Cheeseman, J. R.; Keith, T.; Peterson, G. A.; Montgomery, J. A.; Raghavachari, K.; Al-Laham, M. A.; Zakrzewski, V. G.; Ortiz, J. V.; Foresman, J. B.; Cioslowski, J.; Stefanov, B. B.;

Nanayakkara, A.; Challacombe, M.; Peng, C. Y.; Ayala, P. Y.; Chen, W.; Wong, M. W.; Andres, J. L.; Replogle, E. S.; Gomperts, R.; Martin, R. L.; Fox, D. J.; Binkley, J. S.; DeFrees, D. J.; Baker, J.; Stewart, J. P.; Head-Gordon, M.; Gonzalez, C.; Pople, J. A. *Gaussian 94*, revision D.2; Gaussian, Inc.: Pittsburgh, PA, 1995.

(9) DeMore, W. B.; Sander, S. P.; Golden, D. M.; Hampson, R. F.; Kurylo, M. J.; Howard, C. J.; Ravishankara, A. R.; Kolb. C. E.; Molina, M. J. *Chemical Kinetics and Photochemical Data for Use in Stratospheric Modeling Evaluation #12*; Jet Propulsion Laboratory: Pasadena, CA, January 1997.

(10) Tschuikow-Roux, E.; Faraji, F.; Paddison, S.; Niedzielski, J.; Miyokawa, K. *J. Phys. Chem*. **1988**, *92*, 1488.

(11) Tuazon, E. C.; Atkinson, R.; Corchnoy, S. B. *Int. J. Chem. Kinet*. **1992**, *24*, 639.

(12) Wallington, T. J.; Ball, J. C.; Nielsen, O. J.; Bartkiewicz, E. *J. Phys. Chem*. **1992**, *96*, 1241.

(13) Manning, R.; Kurylo, M. J. *J. Phys. Chem*. **1977**, *81*, 291.

(14) Niki, H.; Maker, P. D.; Savage, C. M.; Breitenbach, L. P. *Int. J. Chem. Kinet*. **1980**, *12*, 1001.

(15) Beichert, P.; Wingen, J. L.; Vogt, R.; Ezell, M. J.; Ragains, M.; Neavyn, R.; Finlayson-Pitts, B. J. *J. Phys. Chem*. **1995**, *99*, 13156.

(16) Wallington, T. J.; Hurley, M. D.; Ball, J. C.; Jenkin, M. E. *Chem. Phys. Lett*. **1993**, *211*, 41.

(17) Notario, A.; Le Bras, G.; Mellouki, A. *J. Phys. Chem*. **1998**, *102*, 3112.

(18) Wu, G.; Van Alsenoy, C.; Geise, H. J.; Sluyts, E.; Vander Veken, B. J. *J. Phys. Chem*. **1995**, *99*, 8589.

(19) Lundell, J.; Rasanen, M.; Raaska, T.; Nieminen, J.; Murto, J. *J. Phys. Chem*. **1993**, *97*, 4577.

(20) Kühne, H.; Ha, T.-K.; Meyer, R.; Günthard, Hs. H. *J. Mol. Spectrosc*. **1979**, *77*, 251.

(21) Tyndall, G. S.; Wallington, T. J.; Potts, A. R. *Chem. Phys. Lett*. **1991**, *186*, 149.

(22) Curl, R. F. *J. Chem. Phys*. **1959**, *30*, 1529.

(23) Bartels, M.; Hoyerman, K.; Langer, U. *Ber. Bunsen-Ges. Phys. Chem*. **1989**, *93*, 423.

(24) Curtiss, L. A.; Ragavachari, K.; Redfern, P. C.; Pople, J. A. *J. Chem. Phys*. **1997**, *106*, 1063.

(25) Good, D. A.; Francisco, J. S. *J. Phys. Chem*., in press.

(26) Tschuikow-Roux, E.; Yano, T,; Niedzielski, J. *J. Chem. Phys*. **1985**, *82*, 65.

(27) Hsu, K. J.; Demore, W. B. *J. Phys. Chem*. **1995**, *99*, 11141.

(28) Scott, A. P.; Radom, L. *J. Phys. Chem.* **1996**, *100*, 16052.